The Journal of Neuroscience, August 1994, 14(8): 4998–5010

Pathway-Specific Variants of AMPA Receptors and Their Contribution to Neuronal Signaling

Indira M. Raman,[1] Su Zhang,[2] and Laurence O. Trussell[2]

[1]Neuroscience Training Program and [2]Department of Neurophysiology, University of Wisconsin–Madison, Madison, Wisconsin 53706

Neurons of the nucleus magnocellularis (nMAG) of the chick express AMPA (α-amino-3-hydroxy-5-methyl-4-isoxazole-propionate) receptors displaying unusually rapid kinetics of desensitization (Raman and Trussell, 1992a). To investigate whether fast AMPA receptors are present in other auditory neurons, we compared the properties of AMPA receptors in auditory as well as nonauditory cells. These included neurons of nMAG, the nucleus angularis, the nucleus laminaris, the cochlear ganglion, the Purkinje cell layer of the cerebellum, the ventral horn of the spinal cord, and the brainstem nucleus of the glossopharyngeal nerve (nclX). Rapid application of glutamate to voltage-clamped outside-out membrane patches indicated that AMPA receptors in the four types of auditory cells had significantly faster kinetics of desensitization than did the three types of nonauditory neurons. Channel kinetics in auditory (nMAG) and nonauditory (nclX) cells were also compared by means of spectral analysis and the time course of current deactivation upon removal of glutamate. Both techniques revealed a burst duration for nMAG channels of 400–500 μsec at room temperature, two to three times shorter than for nclX cells. Single channels in nMAG had a burst duration of 550 μsec and an open time of ≈150 μsec. Miniature excitatory postsynaptic currents of brainstem auditory neurons in slices were also brief, with decay constants of 150–250 μsec at 29–32°C. We demonstrated that the fast kinetics of this AMPA receptor are physiologically important, since cyclothiazide, which reduces desensitization and prolongs synaptic currents, doubled the relative refractory period of orthodromic spikes in nMAG cells in brain slices. We conclude that auditory brainstem neurons express a specialized subtype of AMPA receptors. This "fast" AMPA receptor may be useful in transmitting signals necessary for sound localization.

[Key words: auditory, desensitization, glutamate receptors, cochlear nucleus, chick, AMPA, synapse, hearing]

The diversity of AMPA receptors has recently been demonstrated at both the cellular and the molecular levels. Several structurally distinct AMPA-receptor subunits have been cloned and sequenced, some of which differ in their electrophysiological responses to glutamate and in their distribution throughout the nervous system (reviewed by Seeburg, 1993). Regarding native receptors, neurons can display AMPA receptors with differing physiological properties (e.g., Trussell and Fischbach, 1989; Colquhoun et al., 1992; Hestrin, 1992, 1993; Livsey et al., 1993). Thus, it is possible that variants of the AMPA receptor contribute neuronal properties that are appropriate to the signaling roles of particular pathways. However, unless the types of signals that are transmitted by these neurons are clearly defined, the significance of the responses remains uncertain.

In the auditory pathway of owls, certain neurons are known to respond selectively to certain aspects of sound stimuli; in particular, neurons of the nucleus magnocellularis (nMAG) and the nucleus laminaris (nLAM) encode the temporal properties of sounds, and neurons of the nucleus angularis (nANG) encode the intensity level of sounds (Moiseff and Konishi, 1983; Sullivan and Konishi, 1984; Takahashi et al., 1984). Both timing and intensity cues are used in the localization of sound sources (reviewed by Konishi et al., 1988). The firing patterns characteristic of these neurons in the owl are largely preserved in the chick (Warchol and Dallos, 1990). Thus, the avian auditory system provides a preparation in which receptor properties may be interpreted in the context of signaling needs. The synaptic connections of the first levels of the chick auditory system are depicted in Figure 1. Cochlear ganglion (CG) cells, which are contacted by hair cells of the cochlea, constitute the sole output of the cochlea. Their projections form the auditory nerve and innervate two brainstem nuclei, nMAG and nANG (Parks and Rubel, 1978), which are homologous to parts of the mammalian cochlear nuclei (Boord, 1969; Jhaveri and Morest, 1982). The nMAG neurons bilaterally innervate nLAM neurons, which are also in the brainstem (Ramon y Cajal, 1908b; Jhaveri and Morest, 1982; Young and Rubel, 1983).

In an earlier study (Raman and Trussell, 1992a), we found that the neurons of the nMAG in the chick express AMPA receptors displaying unusually rapid kinetics of desensitization, a feature suitable for maintaining temporally precise patterns of firing (see Discussion). This observation raised the possibility that auditory neurons might have AMPA receptors in which the kinetics are specialized appropriately to the informational content of the signals being transmitted. Accordingly, we have examined the responses of AMPA receptors in CG, nMAG, nANG, and nLAM neurons, representing three levels of auditory processing and two distinct developmental origins, namely, the otic placode and neural tube, and we have compared these responses with those of three types of nonauditory neurons. Here we report that AMPA receptors with fast gating kinetics are

Received Oct. 28, 1993; revised Feb. 3, 1994; accepted Feb. 17, 1994.

L.O.T is supported by a grant from the National Institutes of Health (NS28901) and by the Esther A. and Joseph Klingenstein Foundation. I.M.R. was supported by NRSA GM07507 and is a fellow of the Ford Foundation.

Correspondence should be addressed to Indira M. Raman, Department of Neurophysiology, 285 Medical Sciences Building, 1300 University Avenue, Madison, WI 53706.

characteristic of all the auditory neurons studied, and that these receptors appear to be distinct from the AMPA receptors of nonauditory cells.

Some of these data have been reported in preliminary form (Raman and Trussell, 1993).

Materials and Methods

Cell preparation

Dissociated cells. Neurons from each desired brain region were enzymatically isolated from embryonic chicks between ages E17 and E21, according to the cell dissociation technique described previously (Raman and Trussell, 1992a). For all brainstem and cerebellar regions, brain slices (≈300 μm thick) were cut with a vibratome, and the slices were incubated in enzyme (papain; Worthington, Freehold, NJ, product codes LSOO3126 and LSOO3127); for spinal cord and cochlear ganglion experiments, the entire cord or ganglion was dissected and placed in enzyme. Minor modifications in the period of incubation (15–25 min) or amount of papain (20–40 U/ml) were made according to cell type. Brainstem nuclei, cerebellar cortex, and pieces of lumbar spinal cord were microdissected from the slices with fine tungsten needles. Cochlear ganglia were minced. The tissue was then triturated gently with fine-tipped Pasteur pipettes. After dissociation, the cells were allowed to settle onto a poly-D-lysine–coated coverslip in the recording chamber, which contained bathing solution composed of 140 mM NaCl, 5 mM KCl, 1 mM $MgCl_2$, 3 mM $CaCl_2$, 10 mM HEPES, 1 mM pyruvate, and 20 mM glucose, buffered to pH 7.3 with NaOH. Pyruvate seemed to improve the viability of the neurons during and following the dissociation procedure.

Brain slices. Brain slices from E18–E21 chick embryos were maintained *in vitro* as described previously (Trussell et al., 1993) at 29–32°C, in bathing solution without pyruvate. The methods for obtaining mouse brain slices were similar to those described by Zhang and Oertel (1993). Briefly, CBA or ICR mice, between 14- and 23-d-old, were decapitated and the dissections were performed in warm, oxygenated saline. The medial side of the cochlear nuclear complex was detached with a small surgical scissors, resulting in a slice between 400 and 500 μm thick. The slice was incubated for 1–2 hr in oxygenated saline at 35°C and then transferred to the same type of recording chamber used for the chick brain slices, as described above. The slices were maintained at 29–32°C.

Recording technique

Dissociated cells were maintained in bathing solution. Neurons were voltage clamped in the whole-cell or outside-out patch configurations (Hamill et al., 1981) and held at −70 mV in all experiments unless otherwise mentioned. Junction potentials were accounted for, and corrected holding potentials are indicated in figures. For the patch studies, which used high concentrations of glutamate, 20 μM 6-cyano-7-nitroquinoxaline-2,3-dione (CNQX; Tocris Neuramin, Essex, England) was added to the bathing solution to minimize an excitotoxic effect of agonist on the neurons. Half this concentration of CNQX is sufficient to abolish responses to high concentrations of glutamate (Raman and Trussell, 1992a). Electrodes were pulled from 1.2 mm borosilicate glass, coated with Sylgard (Dow Corning, Midland, MI), and heat polished. For measurements of desensitization and deactivation kinetics in patches and for noise analysis in whole cells, 2–3 MΩ electrodes were used; for single-channel studies in patches, 10–20 MΩ electrodes were used. Electrodes were filled with a solution containing 70 mM Cs_2SO_4, 85 mM sucrose, 4 mM NaCl, 1 mM $MgCl_2$, 10 mM HEPES, and 5 mM BAPTA, buffered to pH 7.3 with CsOH. Agonists [Na-glutamate and *N*-methyl-D-aspartate (NMDA), Sigma, St. Louis, MO; AMPA, Cambridge Research Biochemicals, Wilmington, DE] were dissolved in bathing solution without pyruvate or CNQX ("control solution") and applied as described below.

Outside-out patch studies

Measurements of desensitization and deactivation kinetics required rapid application of agonist-containing solutions. For desensitization studies, solution exchange was accomplished through an array of capillary tubes ("flow pipes") in which solution flow (1.7 ml/min) was gated by three-way solenoid valves. Using this flow system, solution was exchanged with an exponential time constant of 320 μsec for patches and 4 msec for whole cells (Raman and Trussell, 1992a). Desensitization rates were analyzed as described in Raman and Trussell (1992a).

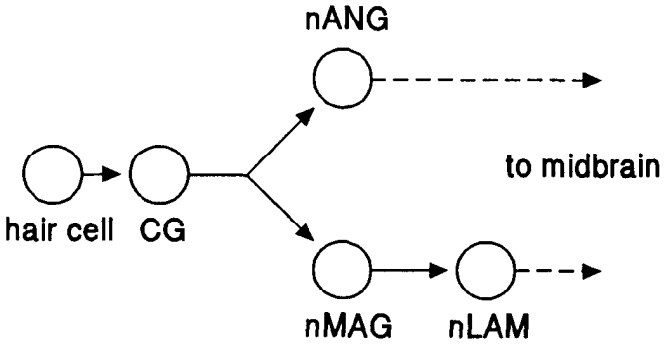

Figure 1. Diagram of the first stages of the auditory system in chicks. Hair cells in the cochlea innervate cochlear ganglion cells (*CG*). CG axons terminate on neurons of the nucleus magnocellularis (*nMAG*) and nucleus angularis (*nANG*). nMAG sends a bilateral projection to neurons of the nucleus laminaris (*nLAM*). nANG and nLAM project to the midbrain.

For the experiments requiring brief applications of agonist, theta glass (World Precision Instruments, Sarasota, FL) was pulled to ≈150-μm-diameter tip and mounted on a piezoelectric translator (Physik Instrumente, Waldbronn, Germany, model 245.30 translator and model P-272 power supply) (Lester et al., 1990). A syringe pump (Harvard Apparatus, South Natick, MA) was used to maintain a continuous stream of control and glutamate-containing (see below) solutions out of the two barrels of the theta glass at approximately 0.4 ml/min. The outside-out patch was positioned near the interface of the control and glutamate streams. Application of voltage to the translator led to a ≈40 μm movement of the theta glass and concomitant movement of the streams over the electrode tip. In this way, the patch could be exposed to glutamate for periods determined by the length of the voltage pulse. The 10–90% rise time of the change in junction potential measured with an open-tipped electrode was 250 ± 30 μsec ($N = 20$), corresponding to an exponential time constant of exchange of about 110 μsec. For the patch experiments, glutamate was dissolved into control solution that had been diluted by 2% with purified water (Lester and Jahr, 1992). After recordings were made from each patch, the electrode tip was cleared by application of pressure to the back of the electrode, and the exchange process was repeated. As the electrode was exposed to the diluted glutamate solution, the change in junction potential was recorded. This procedure enabled precise measurement of the time course of glutamate application to each patch, and indicated that the flow system was reliable. On rare occasions, the junction potential measurements revealed that the patch had been transiently exposed to control solution (probably due to reverberations of either the streams or electrode) during the presumed application of drug, in which case the data from the patch were discarded.

Single-channel activity was examined in the steady state. Ten micromolar or 30 μM glutamate, 30 μM AMPA, or 50 μM NMDA was applied chronically at approximately 0.2 ml/min through the same array of flow pipes used for the desensitization studies. Data were filtered at 5 kHz and saved onto a videotape [via a VR-10B Digital Data Recorder (Instrutech, Elmont, NY) connected to a Mitsubishi videocassette recorder, sampling rate 94.4 kHz]. First, control solution was applied to the patch. Patches with spontaneous channel openings within the first minute were discarded. In quiet patches, the electrode was then moved to the appropriate drug-containing pipe, and channel openings during application of agonist were recorded for 1–2 min.

Following the experiment, 10–20 sec segments of single-channel activity were sampled at 50 kHz via a TL-1 DMA interface, and analyzed with pCLAMP software (Axon Instruments, Foster City, CA). Amplitudes and open times were analyzed separately, according to criteria described by Colquhoun and Sigworth (1983). For open times and burst durations, data were filtered at 5 kHz to improve resolution of brief events. For amplitude analyses, data were filtered at 2 kHz to improve the signal-to-noise ratio. In both cases, threshold was set at about 70% of the maximum open amplitude of the smallest detectable conductance, and the threshold-to-variance ratio was maintained at 3.5 or higher to minimize the inclusion of spurious openings. In the open-time analysis, the threshold detection method was thus optimized to detect the occurrence and duration of individual openings. However, any decrease in open-

channel current by ≈30% was scored as a closure, probably leading to an inclusion of spurious brief closures (gaps) and underestimate of burst durations. Therefore, where possible, a gap duration was estimated from the distribution of the briefest closed times, and open times were reanalyzed by disregarding closures briefer than a critical duration which encompassed the majority (about 99%) of the gaps. In this way, a more accurate estimate of burst duration could be obtained. For open-time measurements, events briefer than the rise time of the system (T_r = 70 μsec) were discarded, and for amplitude measurements, events briefer than 2.5 times T_r (2.5 · T_r = 440 μsec) were discarded.

Whole-cell studies (noise analysis)

A patch pipette filled with 30 μM glutamate was used as a puffer pipette. Initially, whole-cell current (control noise) was recorded (filter frequency, 10 kHz) for about 1 min and stored on videotape. Pressure was then applied to the puffer pipette with a 10 cc syringe. Application of glutamate to a cell invariably resulted in an inward current and an increase in the noise. Pressure was maintained until the current had reached a steady level (glutamate noise) for at least 10 sec, at which time the puffer pipette was removed from the vicinity of the cell and the current was allowed to decline gradually to control levels. This application and removal process was repeated at least twice on each cell.

After recording, the data were played back from the videocassette for analysis (after Anderson and Stevens, 1973; Ascher and Nowak, 1988; Cull-Candy and Usowicz, 1989), and were filtered at 4 kHz with a four-pole Butterworth filter (Krohn-Hite, Avon, MA). The data were digitized with a TL-1 DMA Interface. For determination of channel open times for nMAG neurons, 8 sec segments of control noise and glutamate noise were sampled at 10 kHz with AXOTAPE software. Spectral analysis was performed with computer programs written in AXOBASIC (Axon Instruments). Fast Fourier transforms were performed on each 2048-point segment of control or glutamate noise, giving a 4.88 Hz resolution. For each cell, 38 spectra from each condition were averaged, and the mean control noise spectrum was subtracted from the mean glutamate noise spectrum. The resulting spectra were given as spectral density as a function of frequency. The data were then fitted with 1 or the sum of 2 Lorentzians of the form $S(f) = S(0)/(1 + (2\pi f\tau)^2)$, where $S(f)$ is spectral density in $A^2 \cdot sec$, f is frequency in Hertz, τ represents the open time of the channel in seconds, assuming a model with only one route from a single open state, and $S(0)$ is a constant derived from the mean current amplitude, single-channel conductance, driving force, and open time, and corresponds to the zero-frequency asymptote of the function.

For neurons of the brainstem nucleus of the glossopharyngeal nerve (ncIX) neurons, the initial procedure of filtering at 4 kHz and digitizing at 10 kHz indicated that the power was concentrated at lower frequencies than for nMAG neurons. Therefore, to increase the resolution at low frequencies and provide a better estimate of the zero-frequency asymptote, 16 sec segments of data were filtered at 2 kHz and digitized at 5 kHz, giving a 2.44 Hz resolution. For each cell, 38 control and glutamate noise spectra were analyzed as for the nMAG neurons.

For variance analysis, 25–35 sec segments of noise encompassing the offset of the glutamate-activated current were sampled at 5 kHz. The mean amplitude and variance of successive 1024-point sweeps were determined. Variance (pA^2) was plotted against mean amplitude (pA). Linear regression gave a line whose slope provided an estimate of the single-channel current. From this value, given the driving force (assuming a reversal of 0 mV; Raman and Trussell, 1992b), the mean single-channel conductance could be estimated (Katz and Miledi, 1972; Anderson and Stevens, 1973).

Synaptic events

In slices from both chick and mouse, individual cells were resolved with Nomarski optics. Electrodes were filled with the Cs_2SO_4 solution described above, with 1 mM ATP added. Neurons in slices were voltage clamped with an Axopatch 200A amplifier (Axon Instruments, Foster City, CA) (see Trussell et al., 1993). Spontaneous, miniature postsynaptic currents (mPSCs) were recorded onto videotape (Vetter 3000A, Rebersburg, PA) at 44 kHz, and later played back and redigitized by a computer interface at 30 kHz. During data analysis, mPSCs were identified by eye, either from continuous records or from records extracted by a 10–15 pA threshold setting on an event detector.

Current-clamp recordings were made with an Axoclamp 2A (Axon Instruments, Foster City, CA) in bridge mode. Signals were filtered at 10 kHz before sampling at 25–50 kHz. Cyclothiazide (a gift of E. Lilly Co., Indianapolis, IN) at 40 μM was applied through a pressure pipette located 20 μm from the current-clamped cell. Synaptic events were elicited with a patch pipette that contacted afferent fibers leading to an nMAG neuron. The stimulus pipette was filled with saline, and 40–50 V, 100 μsec stimuli were delivered from an isolated circuit.

Data are given as mean ± SD. Statistical differences were determined with t tests, and significance was taken to be $p < 0.01$.

Results

Neurons were identified on the basis of their location in the brain slice during microdissection and by their dendritic morphology following dissociation. The cell bodies in the brainstem nuclei were highly clustered and, for auditory nuclei, were surrounded by bundles of myelinated axons. Thus, individual nuclei could be easily resolved with a stereo microscope. After enzymatic treatment and trituration, neurons often retained substantial portions of their dendritic arbor. nANG neurons exhibited a variety of sizes and shapes, but were generally multipolar (Ramon y Cajal, 1908b), as shown in the middle panels of Figure 2. nLAM neurons had tufts of dendrites at opposite poles of elongate cell bodies. The length of the cell body and dendritic tufts varied considerably, as illustrated by the two examples in the bottom panels of Figure 2. These morphologies are characteristic of nLAM neurons from the medial and lateral portions of the nucleus (Smith, 1981). As expected from their *in vivo* morphology, neurons dissociated from the nMAG were spherical and adendritic, but occasionally retained a portion of their axon (Fig. 2, top left panel). Neurons of the CG were ovoid or bipolar (Ramon y Cajal, 1908a). In order to control for possible influences of the cell isolation and drug application procedures, nonauditory neurons were also dissociated. These included neurons from the Purkinje cell layer of the cerebellum (Pkj), the brainstem nucleus of the glossopharyngeal nerve (ncIX), and the ventral horn of the spinal cord (vhorn). Purkinje neurons were recognized as large (10–20 μm) cell bodies with a single thick dendrite that occasionally exhibited secondary and tertiary branches. In the ncIX or vhorn, multipolar cells, which composed the majority of neurons in the preparations, were selected for recordings. An ncIX cell is also displayed in Figure 2 (top right panel).

Kinetics of desensitization

The microscopic kinetics of channel gating shape the onset of desensitization of current in response to prolonged exposure to agonist (Raman and Trussell, 1992a). Consequently, the rate of desensitization provides a convenient means to distinguish among AMPA receptors with different channel kinetics. A high dose of glutamate was necessary to assess the maximal rate of desensitization (Trussell and Fischbach, 1989; Smith et al., 1991; Raman and Trussell, 1992a). Accordingly, 10 mM glutamate was applied to each patch for 100 msec by means of a rapid perfusion system. Enzymatic digestion of the NMDA receptor during incubation in papain precluded any contribution of NMDA receptors to the glutamate-activated currents (Akaike et al., 1988; Allen et al., 1988; Raman and Trussell, 1992a). Nevertheless, to verify that the NMDA receptors were indeed inactive, we applied 100 or 300 μM NMDA to patches from nMAG and ncIX under the same recording conditions as the glutamate experiments. No response to NMDA was observed in any patch, despite sensitivity to glutamate or AMPA (N = 5; data not shown).

We measured the amplitudes of peak currents as well as the

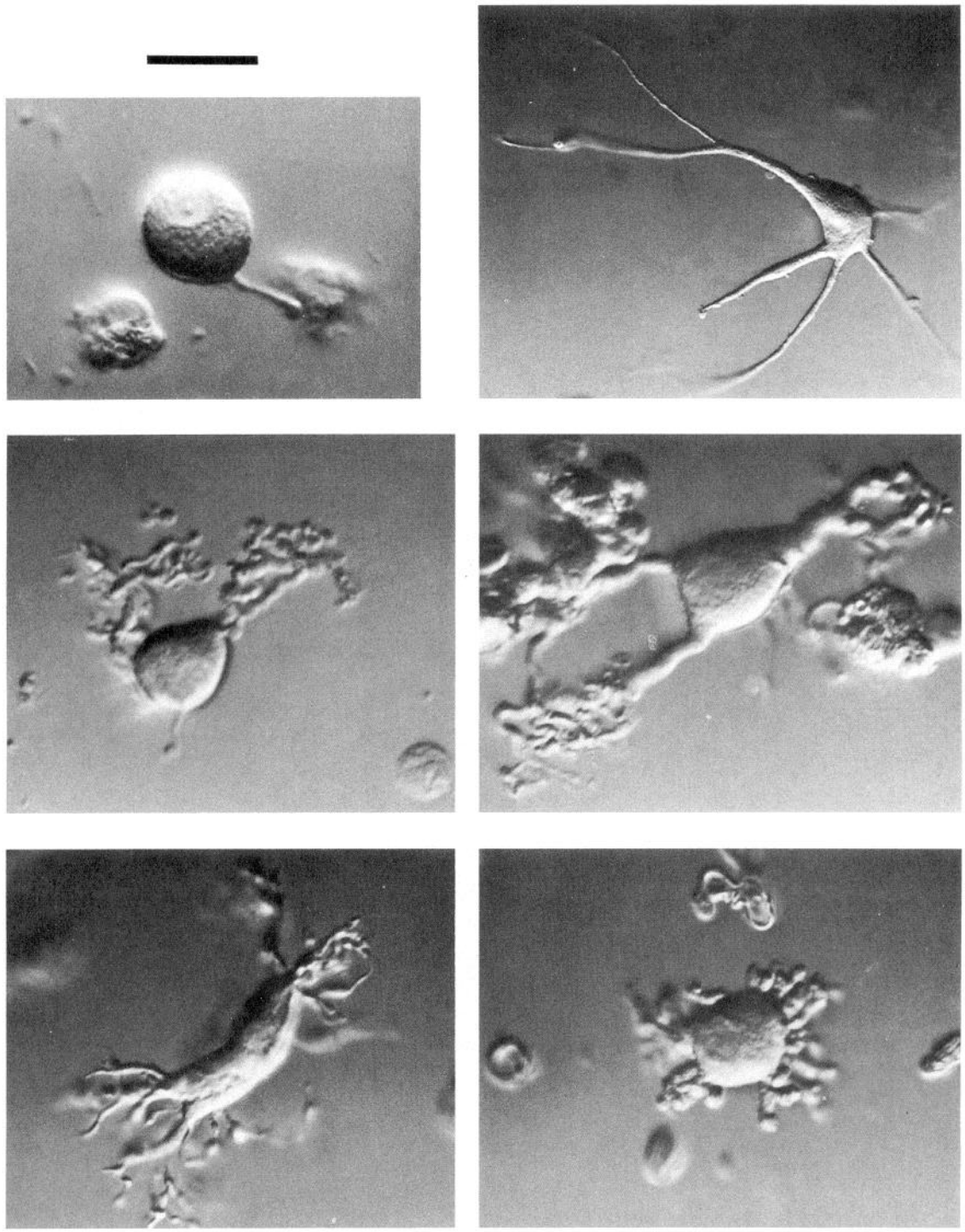

Figure 2. Photomicrographs of dissociated neurons from nMAG (*top left panel*), ncIX (*top right panel*), nANG (*middle panels*), and nLAM (*bottom panels*). *Scale bar*: 40 μm for top right panel; 20 μm for all others.

time course of desensitization for 4–17 neurons from each brain region. The peak amplitudes of the responses are shown in Table 1. Compared to the nonauditory cells, the brainstem auditory neurons exhibited a larger peak current amplitude on average, probably reflecting either a higher density of somatic receptors or a larger single-channel conductance (but see below); however, in no cell type did the decay kinetics vary according to the amplitude of the response.

Figure 3 shows a representative response to glutamate from each neuronal type. In all cell types, glutamate produced an inward current that had a 10–90% rise time between 0.24 and 0.88 msec. Following the peak, the receptors desensitized with a characteristic time course, which varied according to cell type. In auditory neurons (upper traces), the desensitization rates of glutamate-activated currents are higher than the desensitization rates of nonauditory cells (lower traces). The decay constants obtained from single-exponential fits (τ_d) and double-exponential fits (fast component τ_f; slow component τ_s) to the desensi-

Table 1. Amplitudes and decay kinetics of responses in auditory and nonauditory neurons

Region	Amplitude, pA (*N*)	τ_d, msec (*N*)	τ_f, msec (*N*)	τ_s, msec (*N*)	% fast (*N*)
Cochlear ganglion	−64 ± 22 (12)	2.81 ± 0.94 (11)	1.64 ± 0.57 (9)	7.97 ± 4.0 (9)	78 ± 22 (9)
nMAG[a]	−307 ± 153 (13)	1.82 ± 0.58 (11)	0.96 ± 0.22 (10)	3.50 ± 1.22 (10)	76 ± 9 (10)
nANG	−221 ± 182 (17)	2.15 ± 0.86 (17)	1.12 ± 0.39 (11)	4.32 ± 1.28 (11)	71 ± 17 (11)
nLAM	−203 ± 93 (12)	2.30 ± 0.93 (12)	1.42 ± 0.35 (8)	4.59 ± 0.35 (8)	60 ± 26 (8)
ncIX	−65 ± 65 (12)	12.21 ± 4.3 (9)	5.33 ± 2.7 (8)	26.92 ± 13.1 (8)	52 ± 11 (8)
Purkinje cell layer	−36 ± 18 (10)	4.88 ± 0.80 (10)	2.46 ± 1.02 (8)	10.60 ± 4.50 (8)	65 ± 15 (8)
Ventral horn	−36 ± 9 (4)	8.98 ± 4.8 (4)	2.80 ± 0.99 (4)	12.28 ± 4.59 (4)	38 ± 14 (4)

Values are given as mean ± SD. Outside-out patches were voltage clamped at −70 mV, and 10 mM glutamate was applied to each patch by a rapid perfusion system. The decay phase of glutamate-evoked currents was fit with exponentials of the form $I = A_{ext} \cdot e^{(-t/\tau_d)} + I_{ss}$ (single exponential) and, where appropriate, $I = A_f \cdot e^{(-t/\tau_f)} + A_s \cdot e^{(-t/\tau_s)} + I_{ss}$ (double exponential), where I is total current, I_{ss} is the steady-state current, t is time with reference to the onset of the current, A_{ext} is the extrapolated current amplitude at time zero, A_f and A_s are the extrapolated current components of the fast and slow time decay phases, respectively, and τ_f and τ_s as the fast and slow time constants, respectively. For double exponential fits, the percentage of current contributed by the fast phase is given as % fast = $100 \cdot (A_f/(A_f + A_s))$.

[a] nMAG data from Raman and Trussell (1992a).

tizing phase of the glutamate-activated currents, as well as the proportion of the current contributed by the fast component (%fast) are also displayed in Table 1. In most cases, two exponentials provided a better fit than did a single exponential, as illustrated by the double-exponential fits superimposed on the traces in Figure 3. The decay constants τ_d, τ_f, and τ_s are all significantly briefer in brainstem auditory neurons than in nonauditory neurons, except τ_f for nLAM versus Pkj (but note the large difference in the slow components of these two cell types). Furthermore, despite a long τ_s, the τ_d of CG neurons was significantly shorter than that of any nonauditory neuron. These results indicate that rapidly desensitizing AMPA receptors are a shared characteristic of neurons at the early levels of the auditory system. Moreover, rapid kinetics are not an artifact of our experimental procedures, as the nonauditory cells that we examined exhibited significantly slower channel kinetics.

Noise analysis

The differences in the rates of desensitization between auditory and nonauditory neurons raise the possibility that differences may also exist in the rate of closure of AMPA-receptor channels. Therefore, estimates of mean channel open time or burst duration were obtained by spectral analysis of the responses to glutamate in intact cells. nMAG and ncIX neurons were selected as representative auditory and nonauditory neurons, respectively. For these experiments, ncIX neurons with smaller dendritic arbors were selected in order to maximize the adequacy of the voltage clamp. In all cells, 30 μM glutamate activated an inward current that was accompanied by an increase in the current noise. Figure 4*A* shows responses to glutamate in an nMAG and an ncIX neuron. Control spectra were subtracted from glutamate spectra as described in Materials and Methods. Examples of spectra and Lorentzian fits are shown in Figure 4*B*. For nMAG neurons, a single Lorentzian function was generally sufficient to fit the data. The mean time constant estimated from these fits was 0.45 ± 0.12 msec ($N = 6$). In one cell, two Lorentzians, having time constants of 0.26 msec and 1.10 msec, were needed to adequately fit the data. By contrast, all the spectra obtained from ncIX neurons required a sum of two Lorentzians for an adequate fit. The time constants for these were 1.07 ± 0.16 msec (τ_{short}) and 21.86 ± 14.64 msec (τ_{long}) ($N = 4$). The relative contribution of the short and long components was calculated for ncIX neurons as $[S(0)_{short}/\tau_{short}]/[S(0)_{long}/\tau_{long}]$, where $S(0)_{short}$ and $S(0)_{long}$ are the asymptotes of the Lorentzians corresponding to τ_{short} and τ_{long}, respectively. The mean value of this ratio was 19.0 ± 12.7. These results demonstrate that the mean open time or burst duration of AMPA channels in nMAG is indeed briefer than in ncIX.

Variance analysis was also performed on the noise data, in order to compare the mean single-channel conductances of the two cell types. Figure 4*C* shows plots of variance versus mean current for an nMAG (upper) and an ncIX (lower) neuron. In nMAG neurons, the conductance was 3.43 ± 1.06 pS ($N = 6$), and in ncIX, 1.81 ± 0.88 pS ($N = 4$). The difference between the conductances was not significant. This result supports the hypothesis mentioned above, that the difference in mean macroscopic current amplitudes recorded from patches is primarily due to differences in somatic channel density across neuronal types.

Studies of current deactivation

The mean channel open time or burst duration can also be estimated from the time course of current deactivation following rapid removal of agonist (Colquhoun et al., 1992; Hestrin, 1992; Raman and Trussell, 1992a). Theta glass mounted on a piezoelectric translator was used to apply glutamate to outside-out patches from nMAG as well as ncIX neurons. In response to a prolonged (15 msec) pulse of glutamate, currents in nMAG patches rose rapidly and desensitized as in the flow-pipe experiments described above. The time course of desensitization was dose dependent, and the magnitude of the slow component decreased at a lower concentration of glutamate, consistent with

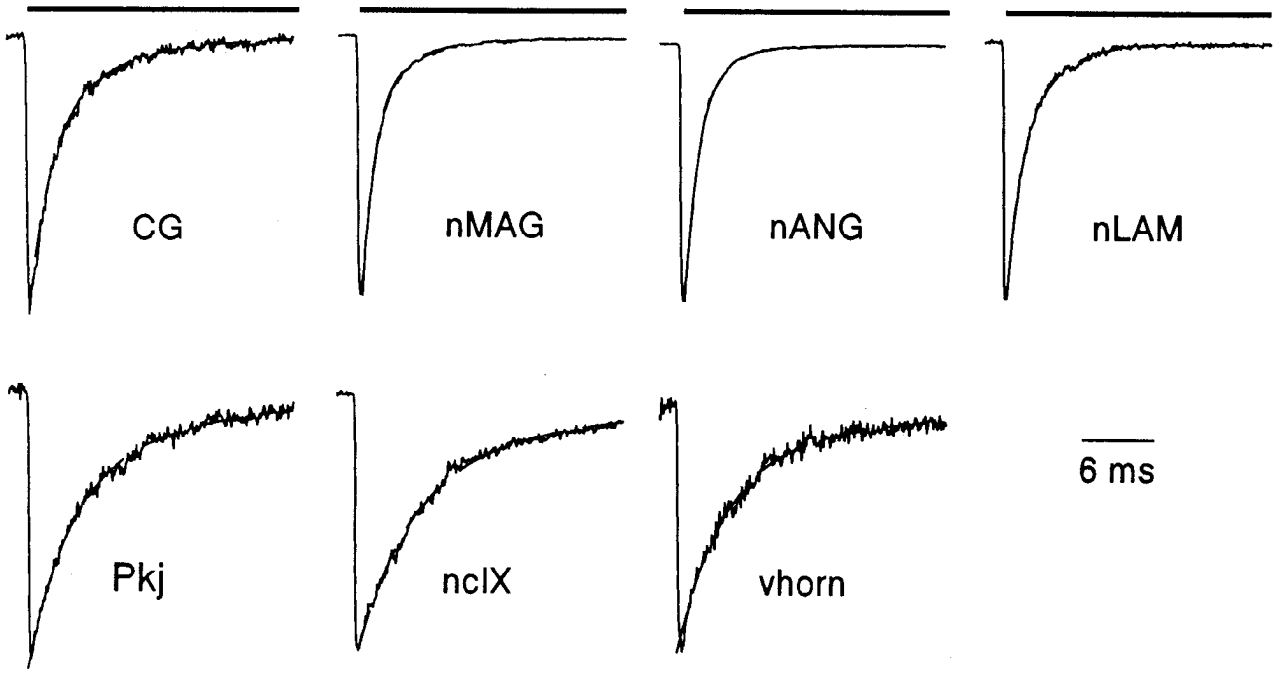

Figure 3. Desensitization rates in auditory and nonauditory neurons: currents evoked by 10 mM glutamate in patches from auditory (*top traces*) and nonauditory neurons (*bottom traces*). The *bars* above the traces indicate the period of glutamate application. Currents have been averaged and normalized to the peak current evoked in each patch. All traces share the same time base. Holding potential, −70 mV. Double exponential fits are superimposed on the traces. Values of τ_{fast} (msec), τ_{slow} (msec), and %fast in these patches are as follows: *CG,* 1.64, 5.54, 67%; *nMAG,* 0.92, 3.30, 80%; *nANG,* 1.10, 3.25, 89%; *nLAM,* 1.07, 3.10, 62%; *Pkj,* 3.27, 10.91, 67%; *ncIX,* 4.15, 16.48, 55%; *vhorn,* 3.69, 12.71, 54%. See text for abbreviations.

flow-pipe experiments (see Raman and Trussell, 1992a). However, due to the better solution exchange provided by the piezoelectric device (see Materials and Methods), the measured desensitization rate was somewhat faster. For 1 mM glutamate, τ_d was 1.40 ± 0.29 msec (N = 8), and for 10 mM glutamate, τ_f was 0.74 ± 0.24 msec and τ_s was 3.14 ± 1.72 msec, with %fast = 74 ± 14% (N = 9). Differences from the flow-pipe measurements were not significant.

A brief (0.8–1.2 msec) pulse of glutamate activated currents in nMAG patches that activated and began to desensitize as for the prolonged pulse. However, when glutamate was removed before desensitization was complete, that is, after 0.8–1.2 msec

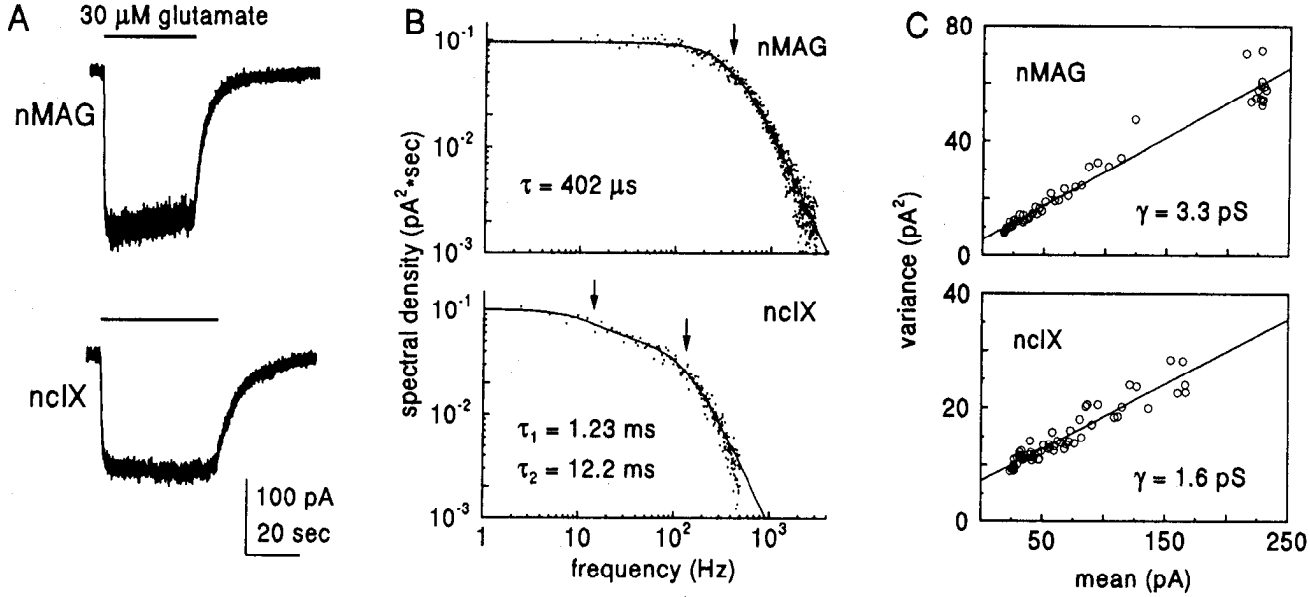

Figure 4. Noise analysis of auditory and nonauditory neurons. *A,* Whole-cell current noise in response to 30 μM glutamate for an nMAG (*top*) and an ncIX (*bottom*) neuron. Holding potential, −70 mV. *B,* Plots of spectral density versus frequency (Hz) for an nMAG and ncIX neuron (different from those in *A*). Data are fitted with a single (*nMAG*) or double (*ncIX*) Lorentzian as described in text. The *arrows* indicate the corner frequencies, at which the spectral density of each Lorentzian has dropped by 50%. The axes are the same in both panels to facilitate comparison. *C,* Plots of variance (pA²) versus mean current (pA) for an nMAG and an ncIX neuron (different from *A*). Regression over the data points gives slopes of 0.24 pA and 0.11 pA, respectively. The single-channel conductance, γ, was calculated assuming a reversal potential of 0 mV.

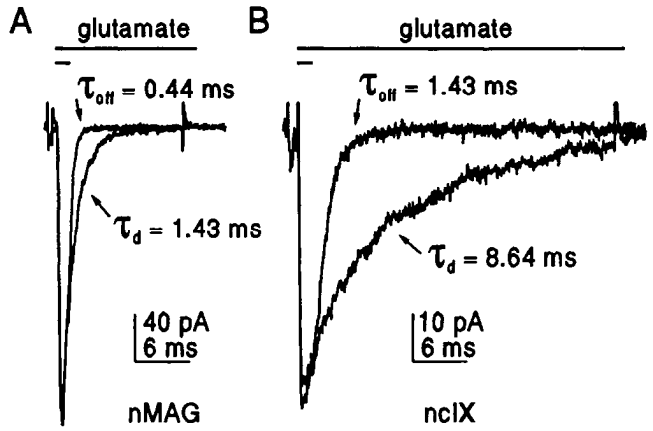

Figure 5. Current deactivation in auditory and nonauditory neurons. *A*, Responses of an nMAG patch to 15 msec and 1.2 msec applications of 1 mM glutamate. *Bars* indicate the duration of exposure to glutamate. The time course of current decay (τ_d) in response to the longer pulse is slower, and reflects the desensitization of the receptors to this dose of glutamate. In response to the briefer pulse, the current offset reflects the time course of the closing of receptors (τ_{off}), which occurs more rapidly. *B*, Responses of an ncIX patch to 30 msec and 1.6 msec applications of 10 mM glutamate. A higher dose was used to maximize the size of the response; longer applications were used to allow measurement of the time course of desensitization. Both *A* and *B* share the same time base to emphasize the differences in the time courses of desensitization and deactivation of the two cell types.

for 1 mM glutamate, the current deactivated even more quickly. Figure 5*A* illustrates the response of an nMAG patch to a long (15 msec) and short (1.2 msec) application of 1 mM glutamate. The time course of current deactivation following the short pulse could be fitted by a single exponential with a time constant (τ_{off}) of 0.50 ± 0.05 msec (N = 8), and was not changed by using 10 mM glutamate (τ_{off} = 0.50 ± 0.13 msec, N = 11) or 300 μM glutamate (τ_{off} = 0.53 ± 0.02 msec, N = 4). This value is shorter than our previous estimate (Raman and Trussell, 1992a) because of the improved exchange time with the piezoelectric device and because the measurements were made at negative holding potentials (Raman and Trussell, 1992b). When similar experiments were performed on patches from ncIX cells, the current deactivation upon removal of 10 mM glutamate was considerably slower, with a τ_{off} of 1.40 ± 0.34 msec (N = 5). An example of deactivating and desensitizing currents in an ncIX patch is shown in Figure 5*B*.

Single-channel studies

To provide a more direct measurement of open time, single-channel recordings were performed on nMAG neurons. Ten or 30 μM glutamate or 30 μM AMPA, but not 50 μM NMDA, activated channels in excised patches. The top five traces in Figure 6*A* show steady-state single-channel currents evoked by chronic application of 10 μM glutamate to an outside-out patch from an nMAG neuron. The bottom two traces show control records from the same patch. Open times were analyzed in five patches. An open-time histogram resulting from measurements made on one patch is shown in Figure 6*B*. On average, single exponential fits to the open-time histograms gave an open time of 145 ± 22 μsec. In four of five patches, two exponentials provided a better fit, with τ_1 = 118 ± 16 μsec and τ_2 = 378 ± 132 μsec, with the briefer component contributing 85 ± 8%.

Although inspection of the single-channel records indicated that most openings occurred in isolation, that is, not as part of a burst structure, three of five patches occasionally showed burst-like events. To select an appropriate gap duration, τ_{crit}, and thereby estimate burst length, the closed-time histograms were examined (Colquhoun and Sigworth, 1983). All five patches showed a major closed time of approximately 15–30 msec. However, this value may have little kinetic relevance, since each patch may have contained more than one channel. The three patches that displayed occasional bursts had a second, briefer closed time of about 100 μsec. These closures probably reflect gaps within bursts. The number and brevity of gaps were probably overestimated (see Materials and Methods); nevertheless, an estimate of burst duration could be obtained by repeating the open-time analysis and ignoring all closures briefer than τ_{crit}, a duration considerably longer than the gaps. The value of τ_{crit} ranged from 0.6 to 1 msec and was selected for each patch such that about 99% of the gaps could be eliminated. All three open-time histograms resulting from this burst analysis required two exponentials for adequate fits. The briefer open time, accounting for 85 ± 2% of the openings, had a duration of 84 ± 9 μsec, and was not significantly different from that measured in these three patches by the analysis in which no τ_{crit} was specified (99 ± 10 μsec). This result reflects the earlier observation that most openings were exceedingly brief, and occurred singly. The longer open time provides an estimate of burst duration, and was 552 ± 64 μsec, significantly different from the first measurement (388 ± 37 μsec). Making τ_{crit} as brief as 300–500 μsec shortened the burst duration measurement to about 440 μsec, and setting τ_{crit} between 1200 and 1600 μsec lengthened the burst estimate to 730 μsec.

Current amplitudes were also measured in the five patches. Although 200–1000 openings were evident in each 20 sec segment of data examined, the majority of events (55–86%) were discarded on the basis of their brief open times (see Materials and Methods), in order to ensure that only fully resolved events were included in the analysis. The amplitude histograms obtained from each patch are shown in Figure 6*C*. Two of the patches contained channels with a relatively high dominant conductance state of approximately 28 pS (histograms A and B), whereas the other three patches had a lower dominant conductance of approximately 18 pS (histograms C–E). The latter three were the patches that exhibited the burst structure described above. We were unable to obtain patches from ncIX neurons of adequate quality to resolve single-channel openings.

Synaptic currents

Miniature PSCs in the nMAG decay exponentially, with time constants (τ_{PSC}) of about 0.2 msec at 33°C (Trussell et al., 1993) and 0.43 msec at room temperature (S. Zhang and L. O. Trussell, unpublished observations). These rates may be a consequence of the rapid kinetics of the AMPA receptors we have studied. We extended the kinetic analysis of synaptic currents to other brainstem auditory nuclei, nANG and nLAM, at 29–32°C. Thirty to 50 mPSCs in each cell were aligned and digitally averaged. The time course of the decay phase of each averaged mPSC was fit with a single exponential function. In the one nANG cell studied, the τ_{PSC} was 0.14 msec, and for the two nLAM neurons the τ_{PSC}s were 0.28 and 0.12 msec. Examples of averaged synaptic events from nMAG, nANG, and nLAM are shown in Figure 7.

To investigate whether AMPA receptors with fast kinetics may also be present in mammalian species, we recorded spontaneous synaptic currents from neurons in slices containing the

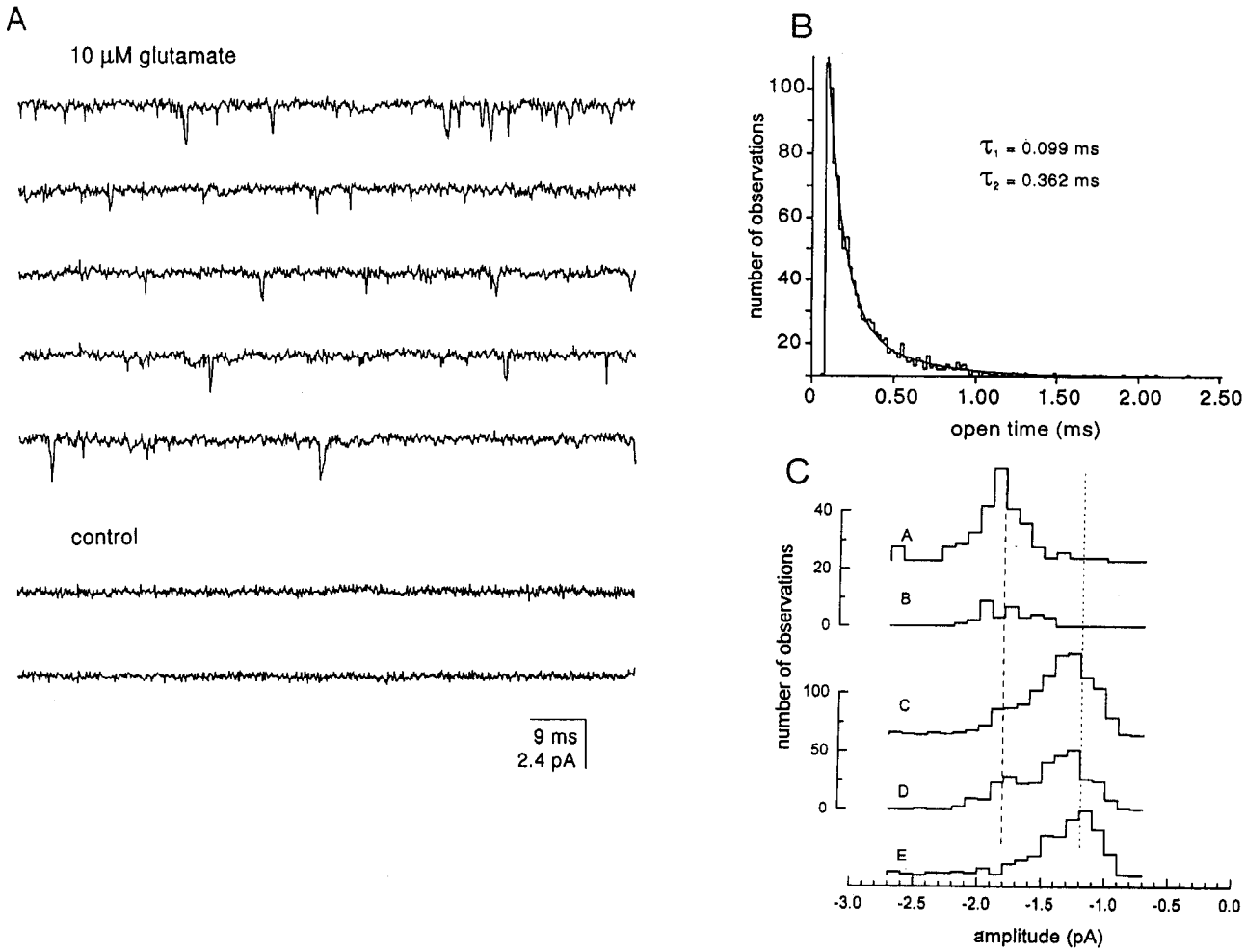

Figure 6. Single-channel analysis of nMAG AMPA receptors. *A,* Consecutive traces of single-channel currents evoked by 10 μM glutamate in an nMAG patch (*top five traces*). *Bottom two traces* are control records. Holding potential, −64 mV. Data are shown filtered at 2 kHz. *B,* Open-time histogram of patch shown in *A*; 1600 openings are included. A double exponential fit is superimposed on the histogram, with a fast time constant (τ_1) of 99 μsec and a slow time constant (τ_2) of 362 μsec. The fast component accounts for 88% of the openings. *C,* Amplitude histograms from five patches. Data are binned at 0.1 pA. All histograms share the same x-axis. The *top y-axis* corresponds to *histograms A* and *B,* and the *bottom y-axis* corresponds to *histograms C–E.* The *vertical lines* at −1.8 pA and −1.2 pA indicate the approximate peaks of the upper two (*dashed line*) and lower three (*dotted line*) distributions. Holding potentials in mV are as follows: *histogram A,* −65; *B,* −67; *C,* −65; *D,* −70; *E,* −64.

anteroventral cochlear nucleus (AVCN) of the mouse. In three neurons, the decay phase of the averaged synaptic event could be described by a single exponential with time constants of 0.15, 0.20, and 0.32 msec. An example of an averaged mPSC from the mouse AVCN is shown in Figure 7. In four other mouse AVCN neurons, we observed a mixture of excitatory synaptic currents, including large fast currents and smaller, slower currents. The two major neuronal cell types in the AVCN are the bushy cells and the stellate cells (Osen, 1969; Wu and Oertel, 1984). Since bushy cells receive their excitatory innervation entirely on their cell bodies, while stellate cells receive excitatory contacts on both their cell bodies and proximal dendrites (Smith and Rhode, 1987, 1989), it is possible that the slower currents represent synaptic events arising from dendritic synapses of stellate cells.

Modulation of receptor kinetics

The rapid kinetics of AMPA receptors in auditory neurons may perform particular functions in information processing (see Discussion). Possibly, a rapid EPSP helps minimize the refractory period for synaptically driven action potentials ("orthodromic spikes"), thus permitting entrainment to high-frequency input. To test this idea, we examined the effect of prolonging the synaptic current on the relative refractory period. The synaptic current was prolonged by bath application of 40 μM cyclothiazide, a drug that reduces AMPA receptor desensitization (Patneau et al., 1993; Trussell et al., 1993; Yamada and Tang, 1993). Action potentials ("direct spikes") were generated by current injection (0.5 nA) into the postsynaptic cell at different intervals following an orthodromic spike. The relative refractory period was defined as the period after the orthodromic spike during which current injection failed to produce a direct spike. Figure 8 (top traces) shows a series of direct spikes in control solutions before and after an orthodromic spike (arrow). The spike obscures the majority of the EPSP, but is followed by a small "after depolarization" generated by activation of both NMDA and AMPA receptors (Zhang and Trussell, 1993). In this case, an action potential was produced 21.3 msec after the orthodromic spike. A marginally suprathreshold stimulus pulse was used to elicit direct spikes, thus making the relative refractory period fairly long.

By contrast, in the presence of cyclothiazide, the synaptic

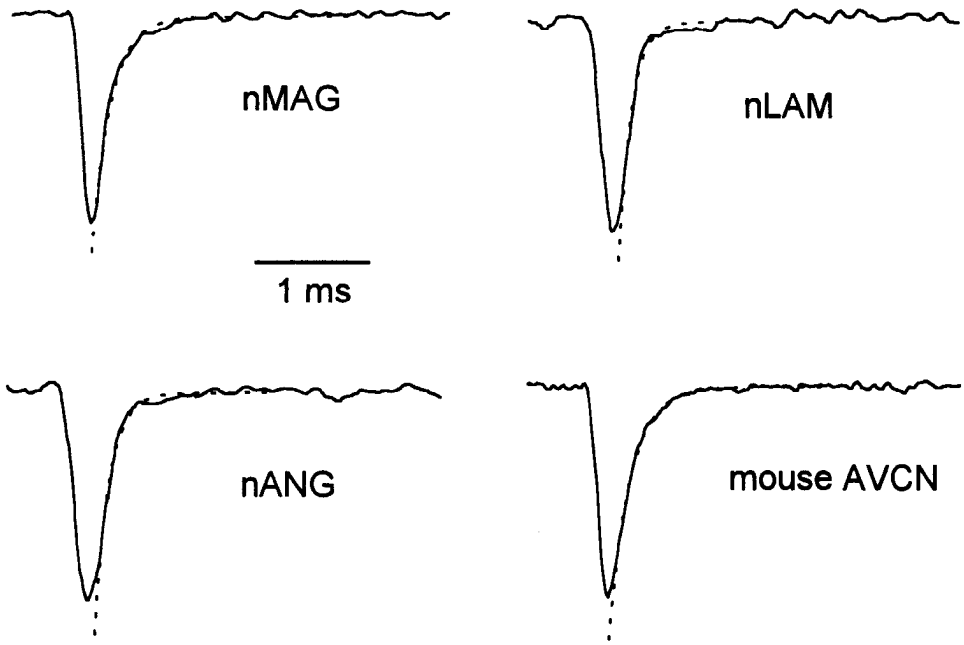

Figure 7. Miniature postsynaptic currents (mPSCs) from nMAG, nANG, and nLAM neurons of the chick and an AVCN neuron of the mouse. Whole-cell recordings were made from neurons in brainstem slices at 29–32°C. Holding potential, −60 mV. mPSCs were averaged and fitted with a single exponential as described in Table 1. The time constants of decay were as follows: nMAG, 0.20 msec; nANG, 0.14 msec; nLAM, 0.12 msec; AVCN, 0.20 msec. Currents are normalized to have comparable peak amplitudes.

potential decayed more slowly, as shown in the lower traces of Figure 8. During this prolonged depolarization, direct spikes could not be elicited, thus extending the refractory period to 37.5 msec. In five cells, the refractory period increased 2.2 ± 0.5-fold in the presence of cyclothiazide. However, 60 μM cyclothiazide had no effect on the refractory period when the conditioning spike was directly evoked (0.5 msec, 1 nA stimulus), rather than synaptically evoked ($N = 4$ cells). Thus, the prolongation of the refractory period is a result of cyclothiazide's action on AMPA receptors. An experiment was also performed in one cell with 5 mM aniracetam (Tang et al., 1991; Vyklicky et al., 1991; Hestrin, 1992), in which the refractory period was prolonged 1.5-fold with orthodromic conditioning spikes (data not shown). The extended synaptic conductance presumably inactivated Na^+ channels by depolarization and shunted the current injected to evoke the direct spikes. Thus, under normal conditions, the brief synaptic current, mediated by AMPA receptors with rapid channel kinetics, may permit nMAG cells to relay signals at higher rates than would be possible with slower channel kinetics.

Discussion

Desensitization studies

AMPA receptors in different parts of the nervous system vary widely in their kinetics of desensitization. To illustrate this point, in Figure 9, mean time constants of desensitization (τ_d) from this study are displayed with τ_ds from several different cell types examined by other authors. Only data obtained using rapid application of glutamate to excised patches are included. We present single exponential fits to the decay phase of currents (except as noted), because not all studies reported two exponential components. The τ_d varies sevenfold, with the fastest rates found in the auditory system. The clustering of auditory cells at one end of this spectrum raises the possibility that auditory neurons express a specialized form of AMPA receptors. Whether receptor properties are conserved within other neuronal pathways remains to be determined.

Channel conductances and open times

The open time of glutamate-gated AMPA-receptor channels in nMAG neurons, measured with three different methods, was also briefer than in other cell types. Comparisons are made only with NMDA-insensitive channels that were activated by glutamate ("AMPA-receptor channels"), except as noted. Single-channel analysis indicated that nMAG AMPA-receptor channels have a typical open time of about 150 μsec. By contrast, neurons in the hippocampus and cerebellum exhibit AMPA-receptor channels with lifetimes between 0.5 and 2 msec (Jahr and Stevens, 1989; Tang et al., 1991; Vyklicky et al., 1991; Wyllie et al., 1993). Bursts of openings in nMAG neurons had a duration of about 550 μsec. The similarity between the single-channel burst time and the spectral and deactivation estimates of open time suggest that the latter two techniques actually provided a measure of burst duration.

Spectral analysis estimated a shorter burst duration of AMPA-receptor channels in nMAG neurons when compared with other chick neurons (ncIX, 1 and 22 msec; spinal neurons, 1.7 msec; O'Brien and Fischbach, 1986) or neurons in the rat cerebellum (2.4 msec, under conditions of active NMDA- as well as AMPA-receptor channels; Cull-Candy and Usowicz, 1989). Finally, deactivation measurements estimate burst times of 2.3–3.0 msec in rat hippocampal neurons (Colquhoun et al., 1992), 2.1 msec in visual cortical neurons (Hestrin, 1992), and 1.4 msec in ncIX neurons, all of which are longer than in nMAG. In both nMAG and ncIX neurons, burst duration estimates from current deactivation in response to high concentrations of glutamate corroborate the single-channel and spectral data. It is significant that the single-channel, spectral, and deactivation estimates of burst duration (550, 450, and 500 μsec, respectively) for nMAG neurons are very close to the decay time constant (430 μsec) of mPSCs in the nMAG at room temperature (Zhang and Trussell, unpublished observations). The correspondence of synaptic and channel kinetics underscores the idea that the range of channel kinetics described here may provide a basis for diversity in

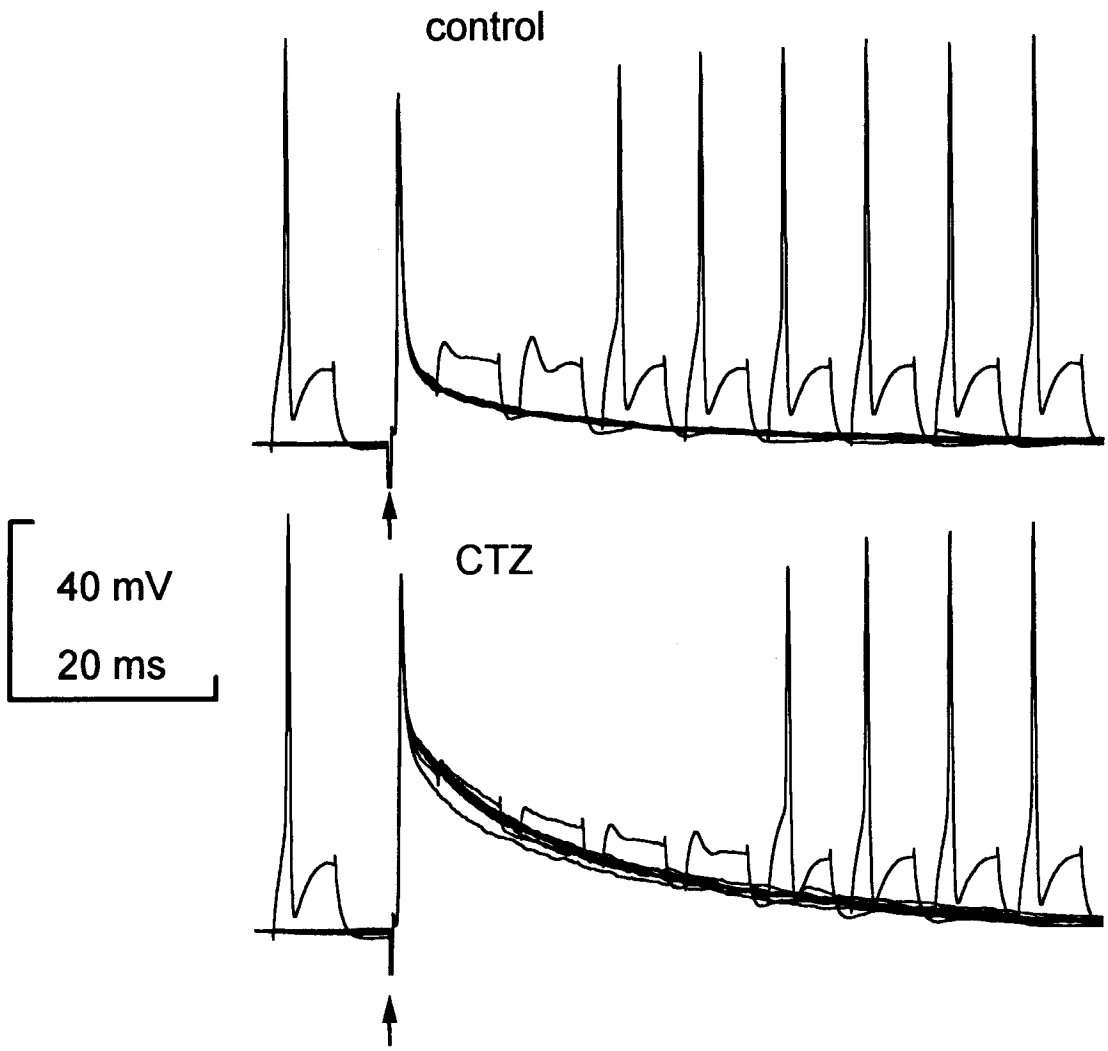

Figure 8. Effect of cyclothiazide on the refractory period following synaptically driven action potentials. Action potentials were elicited either by stimulation of afferent fibers at the time marked by the *arrow* (orthodromic spike), or by injection of 0.5 nA pulses (direct spike). Direct spikes were followed by a brief afterhyperpolarization, whereas orthodromic spikes were followed by a slow relaxation of the membrane potential toward rest. In each panel, direct spikes were elicited before the orthodromic spike and at intervals increasing by 8 msec after the orthodromic spike. The *top panel* shows the responses in control solutions and the *bottom panel* shows responses in the presence of 40 μM cyclothiazide applied to the postsynaptic cell. Resting potential, −68 mV; temperature, 31°C.

synaptic function. Interestingly, the single-channel analysis indicated that the bursts accounted for only ≈15% of the openings. It is unlikely that either the spectral analysis or the deactivation studies, or even the measurements of mPSCs in slices, would resolve an open time on the order of 100 μsec.

Although each patch in our study showed a dominant conductance of approximately 18 or 28 pS, the skewed distribution of the events and inspection of the data traces indicate that more than one conductance level may be present in all the patches. Similarly, other studies of single glutamate-gated channels provide evidence for multiple conductance states between 10 and 40 pS (e.g., Cull-Candy and Usowicz, 1989; Jahr and Stevens, 1989; Wyllie et al., 1993). Additionally, Figure 6*A* reveals that the background noise increased in the presence of glutamate. Although not a finding common to all patches, this result may indicate the existence of an AMPA-receptor channel or state having a smaller conductance. Consistent with this observation, variance analysis indicated a lower mean conductance than that which was measured from single channels, suggesting that lower conductance activity might have been contributing to the overall glutamate-activated current noise. Regarding the comparison of nMAG and ncIX neurons, variance analysis indicates that the particular auditory and nonauditory neurons studied do not differ substantially in their unitary conductances, as measured by this technique.

Significance of receptor kinetics in the auditory system

The interaural timing difference (ITD) pathway, which includes the CG, nMAG, and nLAM, enables localization of sound on the basis of differences in the time of arrival of sound as well as ongoing differences in the phase of sound waves at the two ears (reviewed by Konishi et al., 1988; Yin and Chan, 1988). These neurons must convey accurate temporal information to higher integrative centers, such as the nucleus mesencephalicus pars dorsalis in the midbrain (Moiseff and Konishi, 1983; Conlee and Parks, 1986). Certain characteristics of neurons in the pathway may be particularly suited to this task. Within a cell, impulses must be conducted precisely, with little distortion of

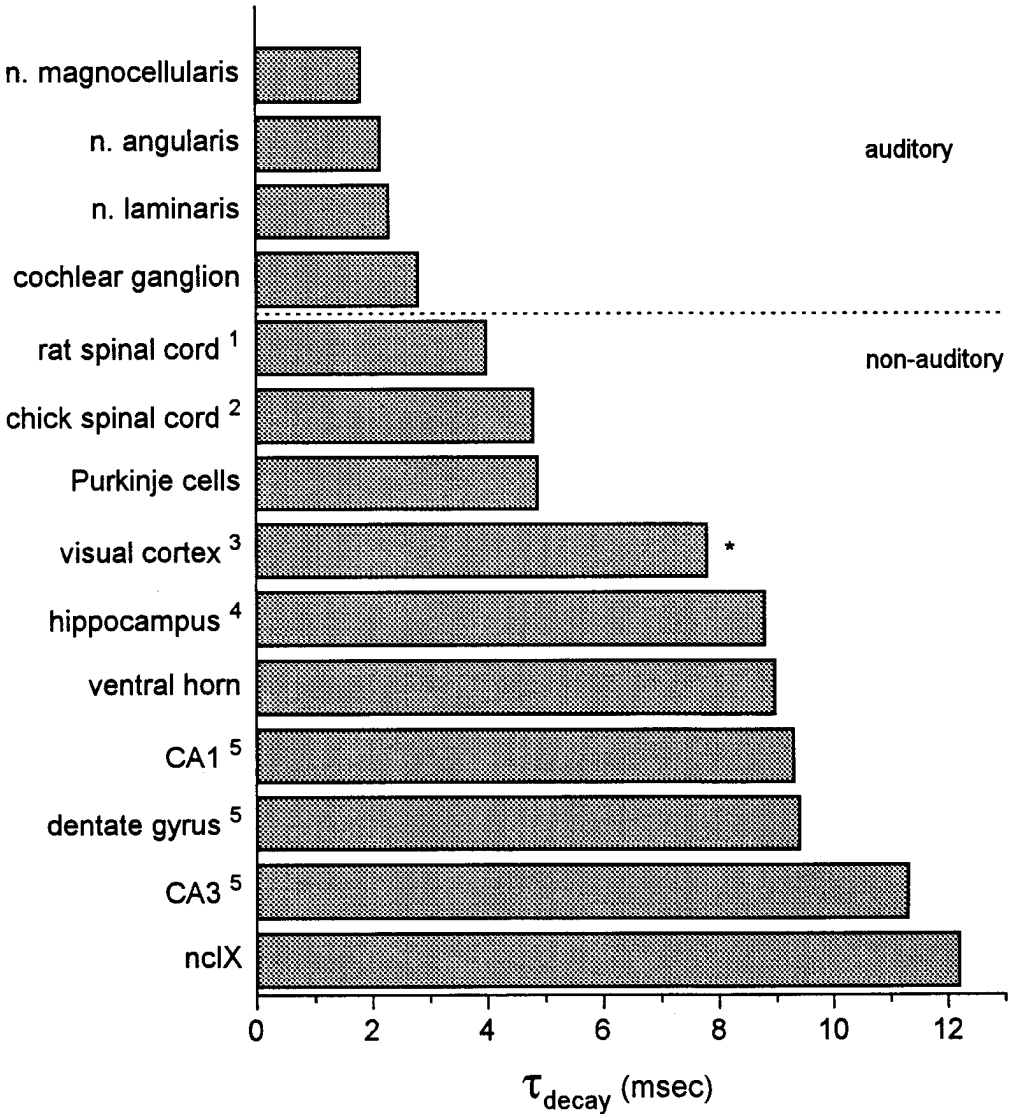

Figure 9. Bar graph comparing time constants of desensitization (single exponential fits, τ_d; *asterisk* indicates τ_f where no τ_d was reported) in various cell types. Sources and glutamate concentrations are as follows: *unmarked*, 10 mM, data from this study; *1*, dissociated from rat, 1 mM (Smith et al., 1991); *2*, cultured from chick, 1 mM (Trussell and Fischbach, 1989); *3*, slices from rat, 10 mM (Hestrin, 1992); *4*, cultured from rat, 1 mM (Patneau et al., 1993); *5*, slices from rat, 1 mM (Colquhoun et al., 1992).

the received signal. Appropriate specializations include minimal cable distortion as a result of somatic innervation, and short membrane time constants (Oertel, 1983; Rothman et al., 1993), both of which are features of the neurons of the nMAG (Jhaveri and Morest, 1982; Zhang and Trussell, unpublished observations). At the level of the synapse, the release of transmitter and the response of the postsynaptic cells must preserve the temporal structure of signals. The kinetics of the receptors themselves may enhance precise synaptic transmission (Raman and Trussell, 1992a). The importance of the kinetics of the receptor to synaptic responses is evident after modulation of receptor gating with cyclothiazide (Fig. 8; Patneau et al., 1992; Trussell et al., 1993; Yamada and Tang, 1993). Reduction of receptor desensitization and, in some cases, lengthening channel open times prolong the synaptic current and synaptic potential. Under normal conditions, the rapid decay of synaptic current may serve to compensate for the large amplitude of the PSC. The evoked PSC in nMAG neurons is typically on the order of 7–8 nA at −20 to −30 mV (Trussell et al., 1993), whereas the sodium current underlying the spike is only 2–3 nA (I. M. Raman and L. O. Trussell, unpublished observations). While the large synaptic current ensures elicitation of a spike, its brevity mimics the Na^+ current and may preserve the shape of the spike as well as minimize the refractory period following synaptically driven spikes. Even for weak synapses, a fast synaptic current is appropriate for the accurate transmission of temporal signals. For cells with more than one subthreshold synaptic input, a brief synaptic current may limit the jitter (asynchrony of input) that can be tolerated in producing a suprathreshold response. Direct demonstration of this reduction in temporal summation requires stimulation of distinct subthreshold inputs to a cell, which was technically unfeasible in our preparation.

Like the nMAG neurons, nLAM neurons exhibit a rapidly desensitizing receptor as well as brief mPSCs, consistent with the proposal that these features are specializations for temporal coding. However, these characteristics are shared by the nANG neurons, which, with the CG cells, participate in the interaural level difference pathway. In this pathway, differences in the intensity of sound at the ears are used as cues to localize sound sources. The role for a fast receptor at a synapse that transmits level information is more difficult to define. Indeed, to encode level information, perhaps a rapid synaptic response is not crit-

ical; thus, it is puzzling that all the nANG patches studied displayed rapid desensitization kinetics, and that the mEPSCs recorded in nANG were so brief. Since the segregation of function is less dramatic in the chick, it may be that these neurons also participate in encoding ITDs. Notably, however, in the barn owl, a number of intrinsic cellular characteristics of nANG neurons distinguish them from nMAG neurons (Sullivan and Konishi, 1984). These physiological differences are less pronounced in the chick (Warchol and Dallos, 1990), but include the following: The nANG neurons have a low spontaneous firing rate (≈20/sec), whereas the nMAG neurons have a high rate of firing (≈90/sec). Although both sets of neurons phase-lock to stimuli from the auditory nerve, nMAG neurons phase-lock to 2 kHz, while nANG neurons phase-lock to only 1 kHz. Furthermore, during a step depolarization, nANG cells fire repeatedly, at rates that increase with the magnitude of the step (Raman and Trussell, unpublished observations), whereas nMAG cells fire a single spike (Zhang and Trussell, 1993). Thus, the intrinsic properties of the nANG neurons may be the dominant factor in enabling them to encode level.

The similarity of AMPA receptors in nMAG and nANG may instead be related to the common excitatory innervation of these regions. Possibly, receptor isoforms are selectively induced by particular types of innervating neurons. In the present case, auditory nerve fibers may provide a signal, either chemical or electrical, which causes either the expression of AMPA-receptor genes encoding a fast kinetic receptor or the covalent modification of slower AMPA-receptor proteins. The particular subunits that compose this "fast" receptor are unknown. However, studies using *in situ* hybridization to identify the mRNA of various AMPA-receptor subunits in the cochlear nucleus of rats indicated that neurons innervated by the auditory nerve expressed GluR2, GluR3, and GluR4, but not GluR1 (Hunter et al., 1993; Sato et al., 1993). It will be interesting to determine whether this pattern of expression has any bearing on the rapidity of the response of AMPA receptors to glutamate.

References

Akaike N, Kaneda M, Hori N, Krishtal OA (1988) Blockade of *N*-methyl-D-aspartate response in enzyme-treated rat hippocampal neurons. Neurosci Lett 87:75–79.

Allen CN, Brady R, Swann J, Hori N, Carpenter DO (1988) *N*-methyl-D-aspartate (NMDA) receptors are inactivated by trypsin. Brain Res 458:147–150.

Andersen CR, Stevens CF (1973) Voltage clamp analysis of acetylcholine produced end-plate current fluctuations at frog neuromuscular junction. J Physiol (Lond) 235:655–691.

Ascher P, Nowak L (1988) Quisqualate- and kainate-activated channels in mouse central neurones in culture. J Physiol (Lond) 399:227–245.

Boord RL (1969) The anatomy of the avian auditory system. Ann NY Acad Sci 67:186–198.

Colquhoun D, Sigworth FJ (1983) Fitting and statistical analysis of single-channel records. In: Single channel recording (Sakmann B, Neher E, eds), pp 191–264. New York: Plenum.

Colquhoun D, Jonas P, Sakmann B (1992) Action of brief pulses of glutamate on AMPA/kainate receptors in patches from different neurones of rat hippocampal slices. J Physiol (Lond) 458:261–287.

Conlee JW, Parks TN (1986) Origin of ascending auditory projections to nucleus mesencephalicus lateralis pars dorsalis in the chicken. Brain Res 367:96–113.

Cull-Candy SG, Usowicz MM (1989) On the multiple conductance single channels activated by excitatory amino acids in large cerebellar neurons of the rat. J Physiol (Lond) 415:555–582.

Hamill OP, Marty A, Neher E, Sakmann B, Sigworth FJ (1981) Improved patch-clamp techniques for high-resolution current recording from cells and cell-free membrane patches. Pfluegers Arch 391:85–100.

Hestrin S (1992) Activation and desensitization of glutamate-activated channels mediating fast excitatory synaptic currents in the visual cortex. Neuron 9:991–999.

Hestrin S (1993) Different glutamate-receptor channels mediate fast excitatory synaptic currents in inhibitory and excitatory cortical neurons. Neuron 11:1083–1091.

Hunter C, Petralia RS, Vu T, Wenthold RJ (1993) Expression of AMPA-selective glutamate receptor subunits in morphologically defined neurons of the mammalian cochlear nucleus. J Neurosci 13: 1932–1946.

Jahr CE, Stevens CF (1989) Glutamate activates multiple single channel conductances in hippocampal neurons. Nature 325:522–525.

Jhaveri S, Morest DK (1982) Sequential alterations of neuronal architecture in nucleus magnocellularis of the developing chicken: a Golgi study. Neuroscience 7:837–853.

Katz B, Miledi R (1972) The statistical nature of the acetylcholine potential and its molecular components. J Physiol (Lond) 224:665–700.

Konishi M, Takahashi TT, Wagner H, Sullivan WE, Carr CE (1988) Neurophysiological and anatomical substrates of sound localization in the owl. In: Auditory function, neurobiological bases of hearing (Edelman GM, Gall WE, Cowan WM, eds), pp 721–746. New York: Wiley.

Lester RAJ, Jahr CE (1992) NMDA channel behavior depends on agonist affinity. J Neurosci 12:635–643.

Lester RAJ, Clements JD, Westbrook GL, Jahr CE (1990) Channel kinetics determine the time course of NMDA receptor-mediated synaptic currents. Nature 346:565–567.

Livsey CT, Costa E, Vicini S (1993) Glutamate-activated currents in outside-out patches from spiny versus aspiny hilar neurons of rat hippocampal slices. J Neurosci 13:5324–5333.

Moiseff A, Konishi M (1983) Binaural characteristics of units in the owl's brainstem auditory pathway: precursors of restricted spatial receptive fields. J Neurosci 3:2553–2562.

O'Brien RJ, Fischbach GD (1986) Characterization of excitatory amino acid receptors expressed by embryonic chick motoneurons *in vitro*. J Neurosci 6:3275–3283.

Oertel D (1983) Synaptic responses and electrical properties of cells in brain slices of the mouse anteroventral cochlear nucleus. J Neurosci 3:2043–2053.

Osen KK (1969) Cytoarchitecture of the cochlear nuclei in the cat. J Comp Neurol 136:453–484.

Parks TN, Rubel EW (1978) Organization and development of the brain stem auditory nuclei of the chicken: primary afferent projections. J Comp Neurol 180:439–448.

Patneau DK, Vyklicky L Jr, Mayer ML (1992) Cyclothiazide modulates excitatory synaptic transmission and AMPA/kainate receptor desensitization in hippocampal cultures. Soc Neurosci Abstr 18:248.

Patneau DK, Vyklicky L Jr, Mayer ML (1993) Hippocampal neurons exhibit cyclothiazide-sensitive rapidly desensitizing responses to kainate. J Neurosci 13:3496–3509.

Raman IM, Trussell LO (1992a) The kinetics of the response to glutamate and kainate in neurons of the avian cochlear nucleus. Neuron 9:173–186.

Raman IM, Trussell LO (1992b) Voltage-dependent kinetics of currents activated by glutamate or kainate. Soc Neurosci Abstr 18:653.

Raman IM, Trussell LO (1993) Pathway-specific variants of AMPA receptors may subserve physiological roles of neurons. Soc Neurosci Abstr 19:720.

Ramon y Cajal S (1908a) Terminación periférica del nervio acústico de las aves. Trab Inst Cajal Invest Biol 6:161–194.

Ramon y Cajal S (1908b) Les ganglions terminaux du nerf acoustique des oiseaux. Trab Inst Cajal Invest Biol 6:195–225.

Rothman JS, Young ED, Manis PB (1993) Convergence of auditory nerve fibers onto bushy cells in the ventral cochlear nucleus: implications of a computational model. J Neurophysiol 70:2562–2583.

Sato K, Kiyama H, Tohyama M (1993) The differential expression patterns of messenger RNAs encoding non-*N*-methyl-D-aspartate glutamate receptor subunits (GluR1-4) in the rat brain. Neuroscience 52:515–539.

Seeburg PH (1993) The molecular biology of mammalian glutamate receptor channels. Trends Pharmacol Sci 14:297–303.

Smith DO, Franke C, Rosenheimer J, Zufall F, Hatt H (1991) Glu-

tamate-activated channels in adult rat spinal cord cells. J Neurophysiol 66:369–378.
Smith PH, Rhode WS (1987) Characterization of HRP-labeled globular bushy cells in the cat anteroventral cochlear nucleus. J Comp Neurol 266:360–375.
Smith PH, Rhode WS (1989) Structural and functional properties distinguish two types of multipolar cells in the ventral cochlear nucleus. J Comp Neurol 282:595–616.
Smith ZDJ (1981) Organization and development of brain stem auditory nuclei of the chicken: dendritic development in n. laminaris. J Comp Neurol 203:309–333.
Sullivan WE, Konishi M (1984) Segregation of stimulus phase and intensity coding in the cochlear nucleus of the barn owl. J Neurosci 4:1787–1799.
Takahashi T, Moiseff A, Konishi M (1984) Time and intensity cues are processed independently in the auditory system of the owl. J Neurosci 4:1781–1786.
Tang C-M, Shi Q-Y, Katchman A, Lynch G (1991) Modulation of the time course of fast EPSCs and glutamate channel kinetics by aniracetam. Science 254:288–290.
Trussell LO, Fischbach GD (1989) Glutamate receptor desensitization and its role in synaptic transmission. Neuron 3:209–218.
Trussell LO, Zhang S, Raman IM (1993) Desensitization of AMPA receptors upon multiquantal neurotransmitter release. Neuron 10: 1185–1196.
Vyklicky L Jr, Patneau DK, Mayer ML (1991) Modulation of excitatory synaptic transmission by drugs that reduce desensitization at AMPA/kainate receptors. Neuron 7:971–984.
Warchol ME, Dallos P (1990) Neural coding in the chick cochlear nucleus. J Comp Physiol [A] 166:721–734.
Wu SH, Oertel D (1984) Intracellular injection with horseradish peroxidase of physiologically characterized stellate and bushy cells in slices of mouse anteroventral cochlear nucleus. J Neurosci 4:1577–1588.
Wyllie DJA, Traynelis SF, Cull-Candy SG (1993) Evidence for more than one type of non-NMDA receptor in outside-out patches from cerebellar granule cells of the rat. J Physiol (Lond) 463:193–226.
Yamada KA, Tang C-M (1993) Benzothiadiazides inhibit rapid glutamate receptor desensitization and enhance glutamatergic synaptic currents. J Neurosci 13:3904–3915.
Yin TCT, Chan JCK (1988) Neural mechanisms underlying interaural time sensitivity to tones and noise. In: Auditory function, neurobiological bases of hearing (Edelman GM, Gall WE, Cowan WM, eds), pp 385–429. New York: Wiley.
Young SR, Rubel EW (1983) Frequency-specific projections of individual neurons in chick brainstem auditory nuclei. J Neurosci 3:1373–1378.
Zhang S, Oertel D (1993) Cartwheel and superficial stellate cells of the dorsal cochlear nucleus of mice: intracellular recordings in slices. J Neurophysiol 69:1384–1397.
Zhang S, Trussell LO (1993) Glutamatergic transmission in the nucleus magnocellularis. Soc Neurosci Abstr 19:276.